Plant Physiol. (1988) 86, 1257–1263
0032-0889/88/86/1257/07/$01.00/0

# Quantitative and Rapid Estimation of $H^+$ Fluxes in Membrane Vesicles[1]

## SOFTWARE FOR ANALYSIS OF FLUORESCENCE QUENCHING AND RELAXATION

Received for publication September 18, 1987 and in revised form January 11, 1988

IAN R. JENNINGS, PHILIP A. REA[2], ROGER A. LEIGH, AND DALE SANDERS*
*Department of Biology, University of York, Heslington, York Y01 5DD, United Kingdom* (I.R.J., P.A.R., D.S.); *and Rothamsted Experimental Station, Harpenden, Hertfordshire AL5 2JQ, United Kingdom* (R.A.L.)

### ABSTRACT

**Proton transport is often visualized in membrane vesicles by use of fluorescent monoamines which accumulate in acidic intravesicular compartments and undergo concentration-dependent fluorescence quenching. Software for an IBM microcomputer is described which permits logging and editing of changes in fluorescence monitored by a Perkin-Elmer LS-5 luminescence spectrometer. An accurate estimate of the instantaneous rate of fluorescence quenching or recovery is then facilitated by least squares fitting of fluorescence data to a nonlinear function. The software is tested with tonoplast vesicles from *Beta vulgaris*. Quenching of acridine orange fluorescence by ATP-driven (primary) transport and relaxation of quenching by $Na^+/H^+$ antiport can both be fitted with single exponential functions. Initial rates of ATP- and $Na^+$-dependent fluorescence changes are derived and can be used for $K_m$ determinations. The method constitutes a simple and efficient alternative to manual analysis of analog fluorescence traces and results in a reliable quantitative measurement of the relative rate of proton transport in membrane vesicle preparations.**

Proton transport plays a central role in energy transduction in plants (11). Primary $H^+$ transport at the energy-coupling membranes of chloroplasts and mitochondria is driven by light and redox potential energy, respectively, and results in the formation of a transmembrane electrochemical $H^+$ gradient ($\Delta\bar{\mu}_{H^+}$).[3] A dissipative flow of protons down this gradient is then coupled to synthesis of ATP. At the plasma membrane and tonoplast, hydrolysis of phosphoanhydride bonds is used to energize $H^+$ transport, with reverse flow of $H^+$ down the resulting ($\Delta\bar{\mu}_{H^+}$. powering transport of other solutes through discrete secondary systems.

Classical electrophysiological techniques have given insight into the kinetics of $H^+$ transport across the plasma membrane of intact plant cells (1) and patch clamp executed in a 'whole cell mode' enables the study of ATP-dependent $H^+$ currents in intact vacuoles (4, 12). More commonly, however, $H^+$ transport is studied in isolated membrane vesicles, whose small size prohibits the electrophysiological approach. Further, the fact that $^3H$ rapidly exchanges with $^1H_2O$ makes radiometric analyses impossible. Optical methods have therefore had to be developed for the routine estimation of the chemical ($\Delta$pH) and electrical ($\Delta\Psi$) components of $\Delta\bar{\mu}_{H}{}^+$ in membrane vesicles (25).

Fluorescent monoamines (*e.g.* acridine orange, quinacrine, and 9-aminoacridine) have been widely applied in plant membrane vesicle studies to monitor both primary (2, 3, 7, 9, 10, 16, 19, 20, 22–24, 26, 27) and secondary (5, 6, 8) $H^+$ translocation. These compounds accumulate intravesicularly in response to an inside-acid pH gradient and this results in a concentration-dependent decrease in the fluorescence signal through dye stacking (25). Inwardly directed $H^+$ pumping may therefore be detected as a decrease in the fluorescence of the amine with time, while, conversely, the activity of some secondary systems can be followed as an increase in fluorescence after imposition of an inside-acid pH gradient. All of the probes concerned are lipophilic in the free base form so that transmembrane equilibration in response to $\Delta$pH is rapid ($\tau < 2$ s). Consequently, changes in fluorescence intensity closely parallel alterations in the magnitude of the pH gradient (for empirical justification see Lee *et al.* [15]; for mathematical justification see Bennett and Spanswick [2]).

With the exception of nonsteady state investigations of photosynthetic systems in the ms time range (14), the kinetics of vesicular transmembrane $H^+$ translocation have been calculated from analog recordings. Thus, rates have been estimated from hand-drawn tangents to curves—a process which is both laborious and errorsome. The problem is particularly acute for secondary transport where the pH gradient is often generated artificially: because of the intrinsic permeability of the membrane to $H^+$ and the high surface area:volume ratio of vesicles, secondary transport is often initiated against a shifting baseline and the signal obtained is short-lived owing to depletion of the limited reserves of intravesicular protons.

Here we report a method for the logging and subsequent analysis of fluorescence data from $\Delta$pH-reporting probes in membrane vesicles. Using tonoplast vesicles from *Beta vulgaris* L. as a model, we show that time-dependent fluorescence change resulting from activation of primary and secondary $H^+$ transport systems can be simply and accurately estimated by least squares fitting of single exponential functions to digitized, stored data. A preliminary report of this work has appeared previously (13).

## MATERIALS AND METHODS

**Hardware.** The software which has been developed enables collection of fluorescence data from a Perkin-Elmer LS-5 (or LS-3) luminescence spectrometer by an IBM-XT microcomputer

[1] Supported by the Agricultural and Food Research Council (Grant AG87/29) and The University of York.

[2] Present address: Rothamsted Experimental Station, Harpenden, Hertfordshire AL5 2JQ, U.K.

[3] Abbreviations: $\Delta\bar{\mu}_{H}{}^+$, transmembrane electrochemical proton gradient; $\Delta$pH, transmembrane pH gradient; $\Delta\Psi$, transmembrane electrical potential difference; BTP, Bis-tris-propane.

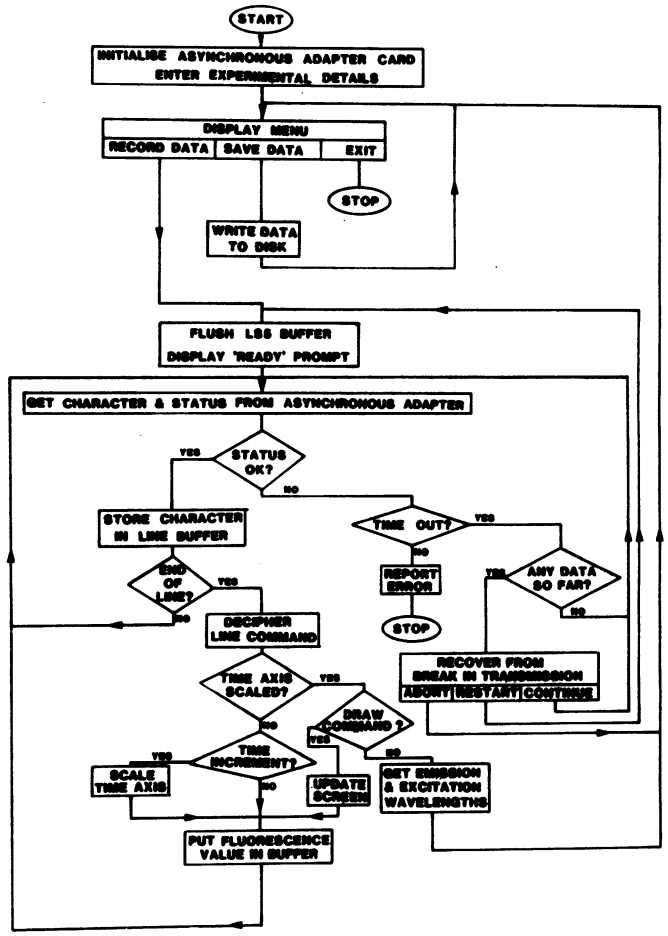


FIG. 1. Flow diagram of LS5. The menu calls the procedures to record or store fluorescence data. The data recording procedure has five stages: (a) Wait for characters from spectrometer (time-out status from synchronous adapter, no data yet received); (b) store characters in line buffer until end of line; (c) count the number of lines until the time axis is incremented and use this to scale the time axis; (d) send fluorescence values already in memory to screen and update the display with incoming data; (e) when the spectrometer sends an 'initiate graph plot mode' character (chr 18), scan through the remaining data and retrieve the emission and excitation wavelengths. Handshaking with the spectrometer is achieved via the computer's Data Terminal Ready signal. This is taken high to receive a character, and then brought low again.

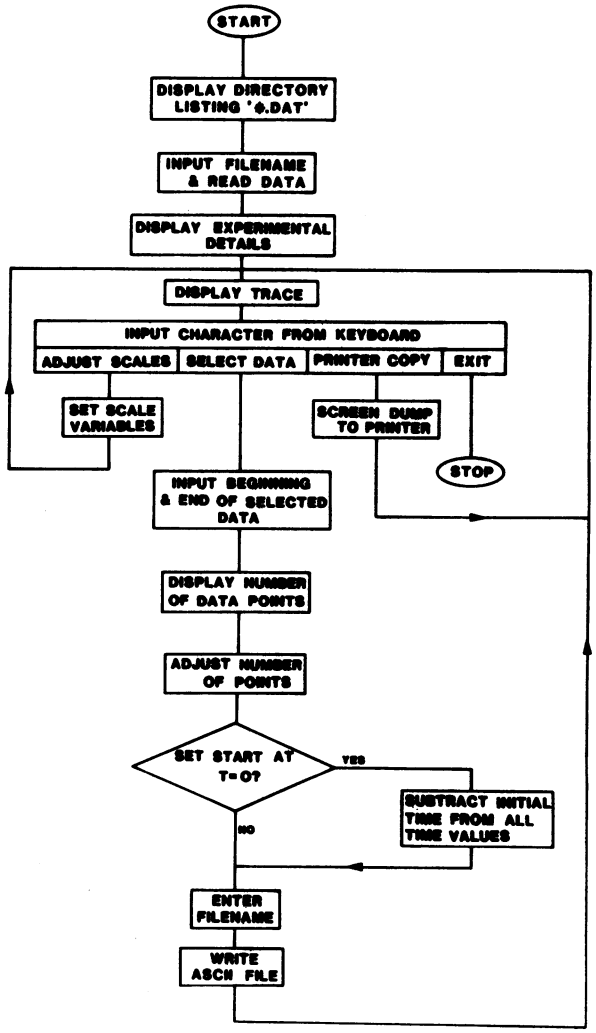


FIG. 2. Flow diagram of LS5EDIT, illustrating review and edit modes. The fluorescence data and note-pad text are read from the integer file created by LS5, the text being deciphered from the integer values. The fluorescence trace displayed on the screen may be sent to the printer using an interrupt-driven routine. This interrupt facility enables further analysis of fluorescence data while the printer is printing.

with a monochrome display. The LS-5 is purchased with an LS-X communications interface which is accessed via an RS 232C port. Input to the microcomputer requires an asynchronous communications adapter and analog display on the monitor is achieved with a Hercules monochrome graphics card. (Hercules look-alike cards may not be compatible, or will require modification if they fail to invert the printer's ACK signal.)

Nonlinear least squares fitting requires a minimum of 256 K of memory and makes use of the 8087 math coprocessor.

**Software.**[4] The software runs with IBM-DOS (Version 2.1, or above). Three programs have been developed: LS5, which logs and generates an on-line display of data from the luminescence spectrometer; LS5EDIT, which allows the user to review stored data and will create a data file compatible for nonlinear least squares fitting; MARQDAT, which uses a commercially available routine to execute least squares fitting.

[4] Those interested in obtaining copies of the software should contact I. R. J. or D. S. at The University of York.

The program structure of LS5 is shown in Figure 1. LS5 is written in Pascal. Recording is initiated and fluorescence intensity scaled at the keyboard of the luminescence spectrometer. Scan speed must be set to 'TIME', but recorder speed is optional: a recorder speed of 0.5 cm/min results in a full screen scaling on the monitor of 20 min, 1 cm/min generates full screen scaling of 10 min, and >2 cm/min corresponds to full screen scaling of 5 min. (This upper limit on time resolution is set by the rate at which horizontal scrolling can be accomplished on the Hercules card.)

Data are sent from the internal buffer of the spectometer via the RS 232C port to the microcomputer at 1200 baud, which corresponds to a sample rate of 10 bi-coordinate data points/s. LS5 deciphers the ASCII plotting codes (normally destined for the Perkin-Elmer GP-100 plotter) to extract the X-Y coordinates of each data point. Relative fluorescence intensity is calculated from the plotting codes by a formula which allows for a fixed ordinate displacement on the GP-100. The time base is also recognized from the plotting codes and assumes the above sampling frequency. In the event that a condensed time base is required for maximum on-line visualization of the trace, values are

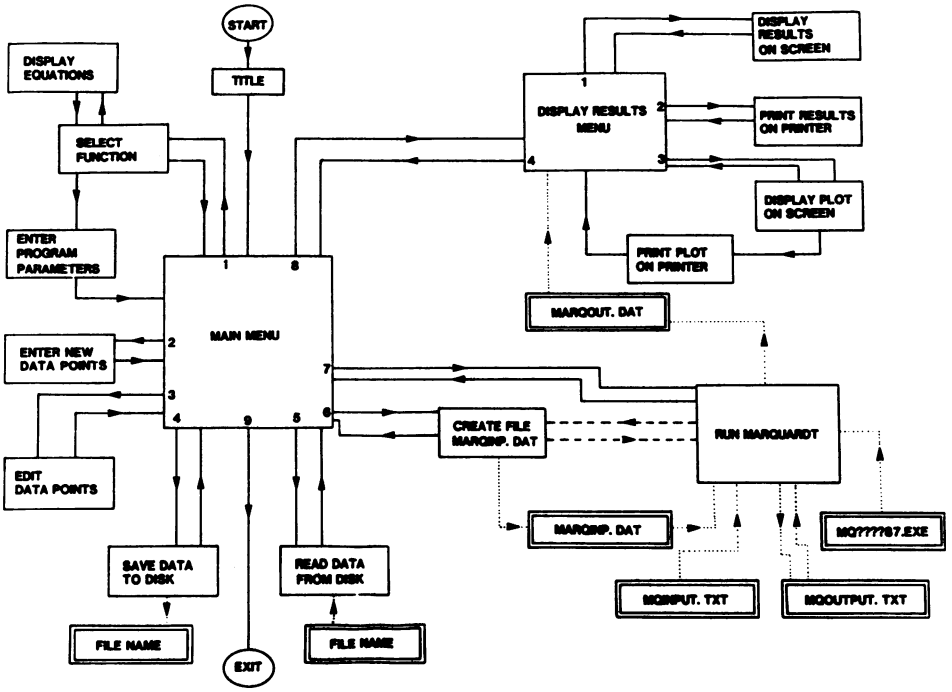


FIG. 3. Flow diagram of MARQDAT. Single-lined boxes and the solid lines connecting them indicate user-interactive pathways; double-lined boxes represent files created by the program, and the dotted lines show pathways followed by the data.

sampled for display. However, all incoming data points are stored directly in memory. The maximum recording time is set by constraints on the array size permitted by Pascal, which corresponds to 40 min continuous recording (*i.e.* 52 kbyte or 2600 s). Since recordings from membrane vesicles rarely exceed 20 min, this limitation is not of practical significance.

Termination of the recording is normally signaled from the keyboard of the spectrometer. The appropriate command from the microcomputer keyboard transfers data from memory to disk, on which they are stored as an integer, rather than as an ASCII, file. Excitation and emission wavelengths are extracted automatically from additional plotting codes sent by the spectrometer once termination is signalled, and these are recorded in the data file. In the event that recording is to be terminated on exceeding the maximum array size, a warning is issued. However transmission breaks (status errors) arising, for example, from faulty hardware connections, are recognized by LS5, thereby enabling continued recording without loss of preexisting data (Fig. 1).

Other facilities of LS5 include a note-pad which appears when the program enters the recording mode. A file-name for recorded data is specified at this stage. The data file-name consists of a six-letter user-specified core mnemonic plus two digits, which begin at 01 and are automatically incremented to prevent overwriting. Details of experimental protocol can also be recorded on the note-pad. After termination of the recording mode of LS5, the user has the option to update the note-pad before the data file is written to disk.

LS5EDIT is also written in Pascal, and its structure is shown in Figure 2. Its purpose is to allow the user to review and edit data logged by LS5 prior to nonlinear least squares fitting. Once a data file is called from disk, the trace is displayed on appropriate axes. Single-key commands facilitate horizontal scrolling of the trace, as well as contraction or expansion of the relative fluorescence scale (full scale limits 100 and 25%, respectively) and time base (full scale limits of 1 and 30 min). This facility enables detailed visual inspection of the trace at the points of interest. A hardcopy of the suitably scaled image is obtained on a dot matrix printer after a screen dump command.

The other major function of LS5EDIT is to write a text (ASCII) file of the data which is compatible for input to MARQDAT. Scaling can also be adjusted in this review mode. A cursor is moved across the screen with single-key commands, and once appropriately positioned, can be used to define the limits of the trace for curve-fitting. The number of data points in the period is displayed. Since the maximum limit on the number of data points for least squares fitting is 200, excess data must be deleted at this stage. Again, this is accomplished with a single key command, which successively selects every second, third, fourth, *etc.* point for inclusion in the text file. The time at the start of the edited trace can be reset to zero, if desired. After specification of a new file name, the text file of the edited data is created. The ASCII file consists of a list of the data point coordinates, prefixed by values for the number of data points and the number of digits per line.

MARQDAT uses the nonlinear least squares fitting algorithm of Marquardt (18) to fit one of a number of functions to the data file created by LS5EDIT. The aim of this procedure is to generate a defined, but purely empirical, expression which accurately describes the data and hence allows determination of instantaneous rates of fluorescence change. User-interactive routines are written in Pascal, while the function-fitting routines are in Fortran. Figure 3 is a flow diagram of MARQDAT. The ASCII file from LS5EDIT can be further edited (point by point) from the main menu. In practice, we have found that the most accurate function for fitting ΔpH-related fluorescence changes is an exponential of the form

$$F = p1\left[p2 - \frac{p3}{\exp[p4(t - p5)]}\right] \quad (1)$$

in which $F$ is fluorescence intensity (%), $t$ is time, and $p1$ through $p5$ are constants derived by the curve fitting. Other functions available include a polynomial.

Since $p1$ is merely a scaling factor, its value can be constrained to 1, with any necessary scaling adjustments appearing proportionally in $p2$ and $p3$. Cases for which an experimental treatment

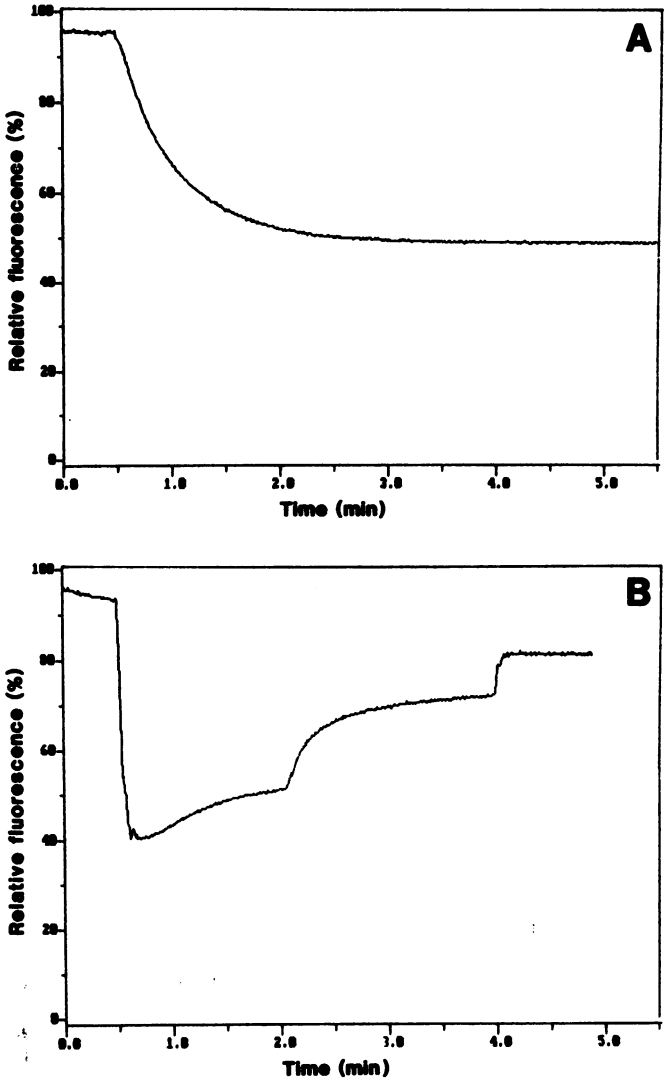


FIG. 4. Screen displays of fluorescence intensity data by LS5. A, Proton pump-dependent quenching of acridine orange fluorescence initiated by addition of 1 mM $MgSO_4$ to a suspension of tonoplast vesicles at 0.48 min; B, tonoplast vesicles (20 $\mu$g membrane protein) subjected to a 'pH jump' from 6.0 to 8.0 at 0.37 min in the presence of acridine orange. At 2.05 min, $Na^+/H^+$ antiport was initiated by the addition of 20 mM $Na_2SO_4$, resulting in rapid recovery of fluorescence; 5 mM $NH_4Cl$ was added at 3.97 min. All other conditions as in "Other Methods."

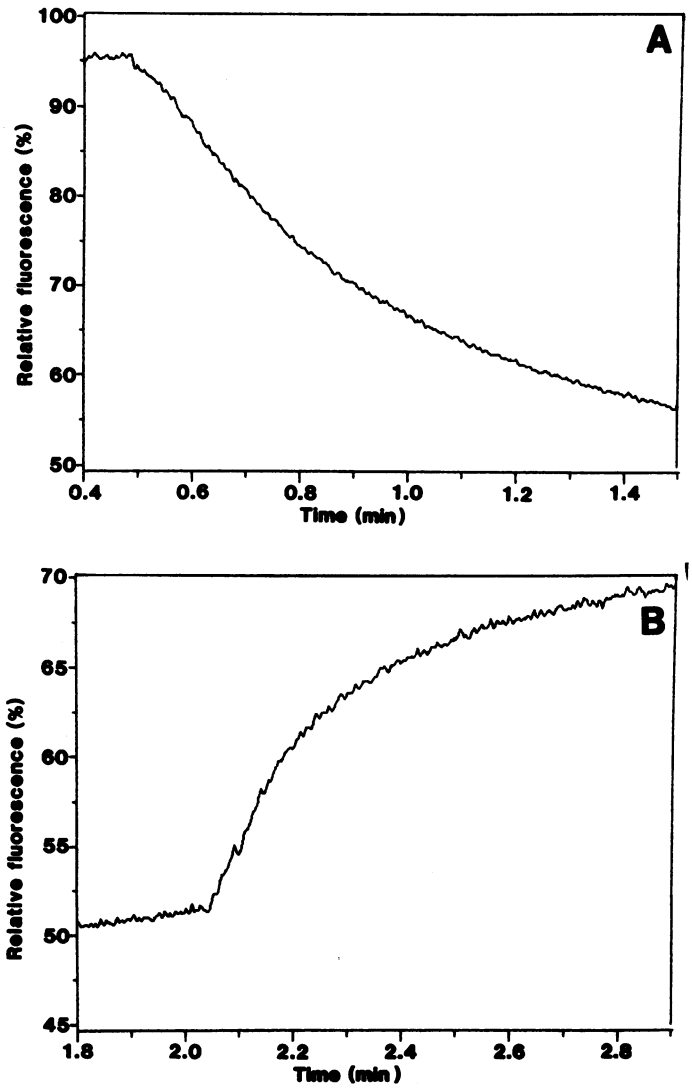


FIG. 5. Scale expansion of selected data from Figure 4 using LS5EDIT in review mode. A, MgATP-dependent fluorescence quenching; B, $Na^+$-dependent fluorescence recovery, focusing on the period immediately before and after the addition of $Na^+$.

generates a shift in baseline fluorescence are accommodated by a finite value of $p5$. Alternatively, constraining $p5$ to the negative of the time at which the treatment begins effectively allows curve fitting without the necessity of redefining the start of the fitting period as time-zero (see LS5EDIT, above). However, no baseline fluorescence shifts were apparent for the particular conditions tested in this paper, and the times at which experimental treatments were initiated have all been reset to zero: this enables $p5$ to be constrained to 0. The resulting simplified form of Eq. 1 is then

$$F = p2 - p3 \cdot \exp(-p4t) \quad (2)$$

in which $p2$ is the final, steady fluorescence, $p3$ is the overall change in fluorescence intensity generated by the experimental treatment, and $p4$ is the rate constant of the change (units: $min^{-1}$). The polarity of $p3$ is negative for fluorescence quenching (proton pumping) and positive for relaxation of quenching. 'Seeding' estimates for $p2$, $p3$, and $p4$ are entered from the main menu, and the number and identity of constrained parameters are specified at this stage.

The file MARQINP.DAT is written on command from the main menu, and is automatically formatted with all information required by the least squares routine. The output file consists of least squares estimates for nonconstrained parameters, together with SE. A graphical display of the data points with the least squares fit is also available and can be obtained on the screen or the printer.

**Other Methods.** The tonoplast vesicles employed for the studies of ATP-dependent $H^+$ translocation (Figs. 4A, 5A, and 6) were taken from the 10/23% (w/w) interface of a sucrose gradient loaded with the microsomal fraction of storage root from red beet (*Beta vulgaris* L.) (24). The vesicles were equilibrated with 0.4 M glycerol and 1 mM DTT buffered to pH 8.0 with 2.5 mM BTP-Mes before the measurement of ATP-dependent $H^+$-translocation. Primary pumping by the tonoplast ATPase was measured in a reaction medium containing tonoplast vesicles (50 $\mu$g membrane protein), 1 mM BTP-ATP, 50 mM KCl, 0.4 M glycerol, and 5 $\mu$M acridine orange (3,6-bis-[dimethylamino]-acridine hydrochloride) buffered to pH 8.0 with 2.5 mM BTP-Mes. $H^+$-translocation was initiated by the addition of 1 mM $MgSO_4$.

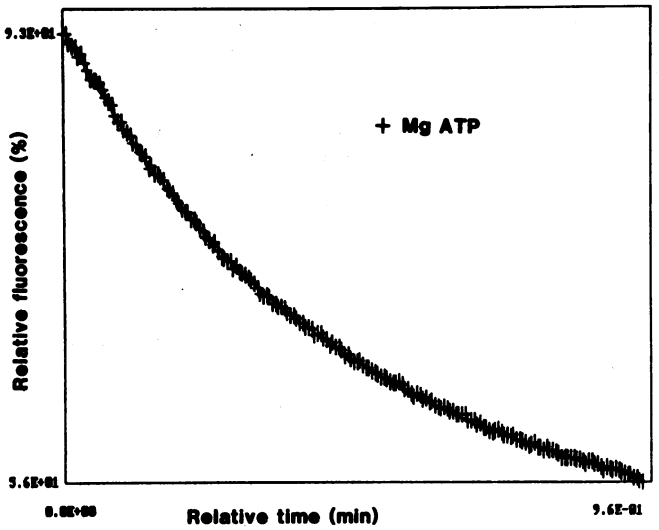


FIG. 6. Nonlinear least squares fit (solid line) of MgATP-dependent fluorescence quenching data (crosses) from Figure 5A. Figure shows graphics output from MARQDAT, after editing of data points by LS5EDIT. Time redefined to 0 at start of trace. Eq. 2 was used for fitting. Least squares estimates (±SE) of $p2$ through $p4$ are: $p2$, 51.8 ± 0.1%; $p3$, −41.5 ± 0.1%; $p4$, 2.21 ± 0.01 $min^{-1}$.

For the experiments demonstrating dissipation of $\Delta$pH by $Na^+/H^+$ antiport (Figs. 4B, 5B, 7 and 8) tonoplast vesicles were prepared on a 6% (w/w) dextran cushion using a combination of the methods of Briskin *et al.* (7) and Rea and Poole (24). The freshly prepared vesicles were resuspended in equilibration medium (0.32 M glycerol, 40 mM K-gluconate, and 1 mM DTT buffered to pH 6.0 with 5 mM BTP-Mes). To ensure thorough intravesicular equilibration the suspension was incubated at 4°C for 2 h before centrifugation at 80,000*g* for 30 min. The pellet was resuspended with equilibration medium to give a membrane protein concentration of 2 to 4 mg/ml.

Artificial transmembrane pH gradients were imposed by diluting 10 $\mu$l of the membrane suspension directly into a fluorimeter cuvette containing 2 ml 0.4 M glycerol, 0.4 mM K-gluconate, 2 $\mu$M valinomycin, and 5 $\mu$M acridine orange buffered to pH 8.0 with 5 mM BTP-Mes. Inclusion of the $K^+$ ionophore valinomycin in the bulk medium and the imposition of a 100-fold $K^+$-gradient served two functions: (a) to stabilize the baseline $\Delta$pH by clamping $\Delta\Psi$ at the equilibrium potential for $H^+$; (b) to minimize electrically coupled $H^+$ fluxes by shunting any substrate-dependent increase in $\Delta\Psi$ through a $K^+$-conductance.

The fluorescence emission of acridine orange was measured at 540 nm at an excitation setting of 495 nm. Slit widths of 5 nm for both excitation and emission were used throughout. The reaction medium was magnetically stirred and thermostatted at 25°C.

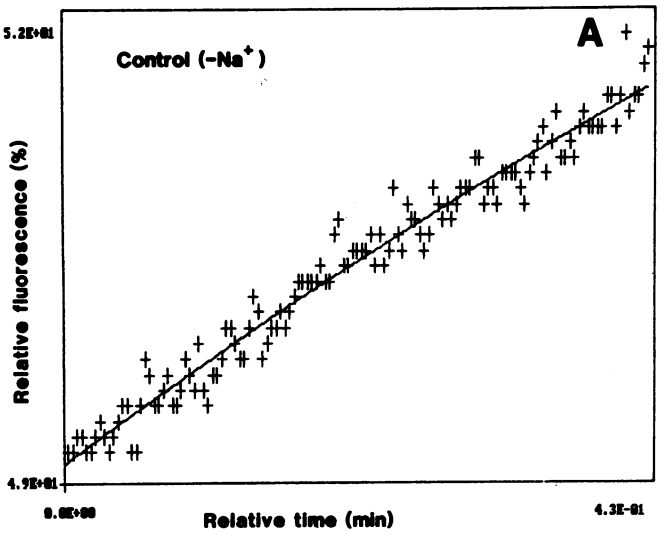


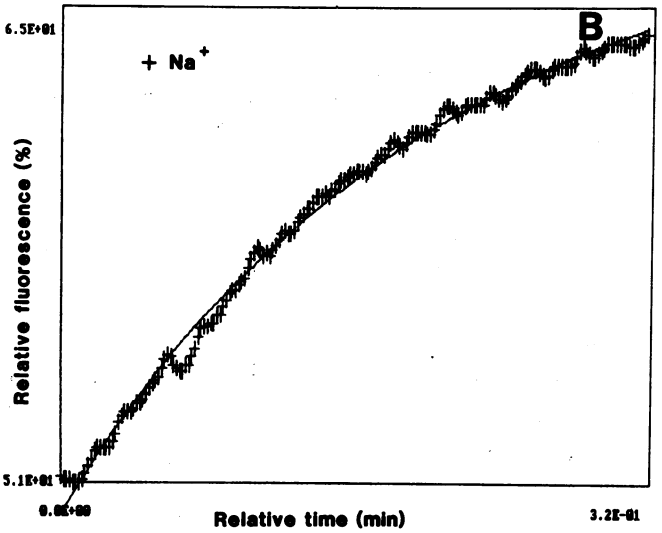


FIG. 7. Nonlinear least squares fits (solid lines) of data (crosses) by MARQDAT after editing by LS5EDIT. Data are from Figure 5B. A, Period of nonspecific proton leakage prior to addition of $Na^+$ (1.75 min to 2.05 min real time), with time redefined to zero by LS5EDIT for the start of the selected period; B, as A, but for the period after $Na^+$ addition (2.05–2.37 min real time). Note different ordinate scales. Fits based on Eq. 2. Least squares estimates (±SE) for $p2$ through $p4$ are as follows:

| Parameter | A | B |
|---|---|---|
| $p2$ (%) | 58.3 ± 3.8 | 68.3 ± 0.2 |
| $p3$ (%) | 8.9 ± 3.8 | 17.9 ± 0.2 |
| $p4$ ($min^{-1}$) | 0.6 ± 0.2 | 5.0 ± 0.1 |

## RESULTS

**LS5 Output.** Typical fluorescence traces, as they appear on screen during recording from a suspension of tonoplast vesicles, are shown in Figure 4. Initiation of $H^+$ pumping by the addition of $Mg^{2+}$ to the ATP-containing buffer at 0.48 min (Fig. 4A) results in a steady decrease in the fluorescence of acridine orange, which plateaus to a steady value of 50.3% at 2.50 min. The plateau represents a steady state between $H^+$ pumping and $H^+$ leakage. ATPase activity can still be measured during this phase but the abstraction of substrate (Mg·ATP) either by the chelation of $Mg^{2+}$, by the addition of EDTA or by the consumption of ATP by the addition of a hexokinase trap to the fluorescence cuvette (*e.g.* Perlin *et al.* [21]; Rea and Poole [24]) causes the rapid efflux of $H^+$ and total abolition of the fluorescence quench.

Figure 4B shows an example of $Na^+/H^+$ antiport. The vesicles are preequilibrated at pH 6.0 ("Other Methods"), and at 0.37 min are added to the fluorescence cuvette containing pH 8.0 buffer. Rapid quenching of the fluorescence of acridine orange from 95 to 41% reflects the imposition of an artificial, inside-acid $\Delta$pH of 2 units. A period of spontaneous partial recovery of the fluorescence then ensues. Sodium/$H^+$ antiport (5) is initiated by the addition of 20 mM $Na_2SO_4$ 2.05 min after the start of the recording This results in a large increase in the rate of fluorescence recovery, consistent with the exit of intravesicular

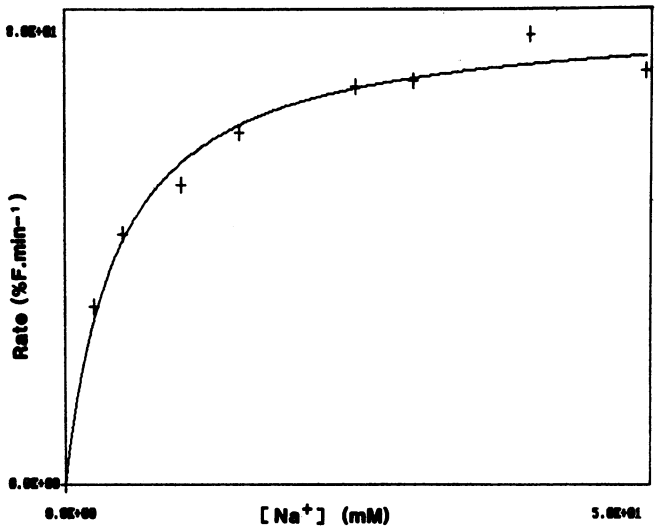


FIG. 8. Velocity-concentration plot derived from the initial rates of fluorescence intensity recovery on addition of $Na^+$ to membrane vesicles. Each point represents an estimate of the rate of $Na^+$-dependent fluorescence recovery obtained using MARQDAT. The solid line is a least squares fit, also derived from MARQDAT, according to the Michaelis-Menten equation. The estimated $K_m$ and $V_{max}$ values are 4.6 ± 0.6 mM and 83.8 ± 2.4%·min$^{-1}$, respectively.

$H^+$ in exchange for extravesicular $Na^+$. The decline in the recovery rate with time reflects the progressive dissipation of the driving force on $Na^+/H^+$ antiport. Addition of 5 mM $NH_4Cl$ at 3.97 min confirms that most of the observed quench is ΔpH-related since this uncoupler causes a further, very rapid, increase in the fluorescence.

**LS5EDIT Output.** LS5EDIT, operating in review mode, facilitates viewing of the periods of interest from the traces in Figure 4. Thus, the changes in relative fluorescence before and after the initiation of ATP-dependent $H^+$ pumping and $Na^+/H^+$ antiport are displayed in Figure 5, A and B, respectively.

The time periods over which least squares fitting is to be performed are then selected, and for the example of $H^+$ pumping in Figure 5A the period from 0.53 to 1.49 min is chosen. (This choice of time span ignores the first 3 s after ATP addition, during which dF/dt is attenuated by the nonlinear dependence of quenching on ΔpH at low values of ΔpH—a point which can be appreciated by reference to Eq. 3 in "Discussion.") Of the resultant 576 data points, 192 (every third point) are used for the creation of the data file for MARQDAT. In the case of $Na^+/H^+$ antiport, the periods before and after addition of $Na^+$ must both be considered, since the control relaxation is significant. The respective time spans selected for analysis are 1.75 to 2.05 min and 2.05 to 2.37 min, respectively. The number of data points is reduced by a factor of 2 in the former case only. Time is redefined to 0 at the start of all selected time spans.

**MARQDAT Output.** In the present examples, the aim of MARQDAT is to provide a quantitative estimate of the initial rates of $H^+$ transport via the $H^+$-ATPase and the $Na^+/H^+$ antiporter. The results of nonlinear least squares fitting of Eq. 2 to the fluorescence data on initiation of $H^+$ pumping are shown in Figure 6. Estimates of the parameters $p2$ through $p4$ are given in the figure legend. The initial rate of MgATP-dependent fluorescence quenching is calculated as the first derivative of Eq. 2 ($= p3 \cdot p4 \exp[-p4t]$), taken at $t = 0$, resulting in a value of (−) 91.8% F·min$^{-1}$.

Figure 7 shows the results of MARQDAT fits of fluorescence data before and after addition of $Na^+$. The least squares estimates of the parameters, again based on Eq. 2, are given in the figure legend. To obtain the initial rate of $Na^+$-dependent fluorescence recovery, the first derivative of the control curve (Fig. 7A) is computed at 0.43 min (2.05 min real time) and subtracted from the first derivative of the $+Na^+$ curve (Fig. 7B), taken at $t = 0$ (also 2.05 min real time). The resultant rate of $Na^+$-dependent fluorescence recovery is (89.4 − 4.1) = 85.3% F·min$^{-1}$.

**Construction of Velocity-Concentration Plots.** The results of a series of experiments in which antiport was initiated by the addition of various $Na^+$ concentrations are shown in Figure 8. The solid line shows a fit generated by MARQDAT according to the Michaelis-Menten equation. The $K_m$ and $V_{max}$ values for $Na^+$-dependent fluorescence recovery were 4.6 mM and 83.8% F·min$^{-1}$, respectively.

## DISCUSSION

The software described here enables even the casual user to undertake quantitative analyses of the kinetics of $H^+$ transport in membrane vesicles using fluorescent probes. The conventional method of estimating the initial rate of fluorescence quenching or recovery from a hand-drawn tangent to a nonlinear analog trace is subject to an error of as much as ±25%, depending on the scaling of the trace. The present method, on the other hand, utilizes the inherently nonlinear features of the fluorescence function to generate a least squares fit which can be accurately differentiated with respect to time. One word of caution is necessary, however: it is essential to ensure, through visual inspection of the fitted curve, that the original data have been accurately fitted over the period of interest. For this reason, a range of functions is available for curve-fitting. The particular function used is of less importance than the values which emerge from the empirical fit.

Fluorescence quenching of the monamine dyes can be converted to ΔpH values if calibrated by pH jumps of defined magnitude. It can be shown, both theoretically and experimentally, that the pH gradient is well described as

$$\Delta pH = \log\left[\frac{Q}{(100-Q)}\right] + \log\left[\frac{V_o}{V_i}\right] \quad (3)$$

where $Q$ is the fluorescence quenching (%) and $V_o$ and $V_i$ correspond to the volumes of the extravesicular and intravesicular phases respectively (2, 15). Furthermore, measurements of intravesicular buffer capacity (units: μmol $H^+$·pH unit$^{-1}$·mg protein$^{-1}$) potentially enable the rates of fluorescence quenching and recovery to be expressed directly as μmol $H^+$·mg protein$^{-1}$·min$^{-1}$ (17, 21). In principle, then, the statistically derived estimates of the rate and extent of fluorescence quenching constitute an important first step in the accurate evaluation of both the thermodynamic and kinetic parameters associated with primary and secondary $H^+$-translocation. Although we have concentrated on changes in ΔpH mediated by primary and secondary $H^+$-translocation, the software is equally applicable to fluorescent dyes which monitor $\Delta\Psi$ (25).

An overriding virtue of this method for the quantitation of transport-related changes in $\Delta\bar{\mu}_{H^+}$ is its cost. The microcomputer and associated hardware may be purchased for little more than the price of the GP-100 printer, and are considerably cheaper than the Perkin-Elmer data station to which the LS-5 luminescence spectrometer may also be interfaced. The software is also simple to use and, with practice, facilitates estimation of initial rates more rapidly than is possible by the analysis of analog data.

### LITERATURE CITED

1. BEILBY MJ 1984 Current-voltage characteristics of the proton pump at *Chara* plasmalemma: I. pH dependence. J Membr Biol 81: 113–125

2. BENNETT AB, RM SPANSWICK 1983 Optical measurements of $\Delta pH$ and $\Delta\Psi$ in corn root membrane vesicles: kinetic analysis of $Cl^-$ effects on a proton-translocating ATPase. J Membr Biol 71: 95–107
3. BENNETT AB, RM SPANSWICK 1983 Solubilization and reconstitution of an anion-sensitive $H^+$-ATPase from corn roots. J Membr Biol 75: 21–31
4. BENTRUP F-W, M GOGARTEN-BOEKELS, B HOFFMANN, JP GOGARTEN, C BAUMANN 1986 ATP-dependent acidification and tonoplast hyperpolarization in isolated vacuoles from green suspension cells of *Chenopodium rubrum* L. Proc Natl Acad Sci USA 83: 2431–2433
5. BLUMWALD E, RJ POOLE 1985 $Na^+/H^+$ antiport in isolated tonoplast vesicles from storage tissues of *Beta vulgaris*. Plant Physiol 78: 163–167
6. BLUMWALD E, RJ POOLE 1986 Kinetics of $Ca^{2+}/H^+$ antiport in isolated tonoplast vesicles from storage tissue of *Beta vulgaris* L. Plant Physiol 80: 727–731
7. BRISKIN DP, WR THORNLEY, RE WYSE 1985 Membrane transport in isolated vesicles from sugarbeet taproot: isolation and characterization of energy-dependent, $H^+$-transporting vesicles. Plant Physiol 78: 865–870
8. BRISKIN DP, WR THORNLEY, RE WYSE 1985 Membrane transport in isolated vesicles from sugarbeet taproot. II. Evidence for a sucrose/$H^+$-antiport. Plant Physiol 78: 871–875
9. CHANSON, A, J FICHMANN, D SPEAR, L TAIZ 1985 Pyrophosphate-driven proton transport by microsomal membranes of corn coleoptiles. Plant Physiol 79: 159–164
10. GABATHULER R, RE CLELEND 1985 Auxin regulation of a proton translocating ATPase in pea root plasma membranes. Plant Physiol 79: 1080–1085
11. HAROLD FM 1986 The Vital Force: A Study of Bioenergetics. Freeman, New York
12. HEDRICH R, UI FLÜGGE, JM FERNANDEZ 1986 Patch-clamp studies of ion-transport in isolated plant vacuoles. FEBS Lett 204: 228–232
13. JENNINGS, IR, D SANDERS 1986 A microcomputer-based system for recording and analysis of fluorescence signals reporting $\Delta\mu_{H+}$ in membrane vesicles. Plant Physiol 80: S-136
14. JUNGE W, YQ HONG, LP QIAN, V VIALE 1984 Cooperative transient trapping of photosystem II protons by the integral membrane portion ($CF_0$) of chloroplast ATP-synthase after mild extraction of the four-subunit catalytic part ($CF_1$). Proc Natl Acad Sci USA 81: 3078–3082
15. LEE HC, JG FORTE, D EPEL 1982 The use of fluorescent amines for the measurement of pH: application in liposomes, gastric microsomes, and sea urchin gametes. *In* R Nuccitelli, DW Deamer, eds, Intracellular pH: Its Measurement, Regulation and Utilization in Cellular Functions, Alan R Liss, New York pp 135–160
16. LEW RR, RM SPANSWICK 1985 Characterization of anion effects on the nitrate-sensitive ATP-dependent proton pumping activity of soybean (*Glycine max* L.) seedling root microsomes. Plant Physiol 77: 352–357
17. MALONEY PC 1979 Membrane $H^+$ conductance of *Streptococcus lactis*. J Bacteriol 140: 197–205
18. MARQUARDT DW 1963 An algorithm for least squares estimation of non-linear parameters. J Soc Indust Appl Math 11: 431–441
19. METTLER IJ, S MANDALA, L TAIZ 1982 Characterization of *in vitro* proton pumping by microsomal vesicles isolated from corn coleoptiles. Plant Physiol 70: 1738–1742
20. O'NEILL SD, RM SPANSWICK 1984 Solubilization and reconstitution of a vanadate-sensitive $H^+$-ATPase from the plasma membrane of *Beta vulgaris*. J Membr Biol 79: 231–243
21. PERLIN DS, MJD SAN FRANCISCO, CW SLAYMAN, BP ROSEN 1986 $H^+$/ATP stoichiometry of proton pumps from *Neurospora crassa* and *Escherichia coli*. Arch Biochem Biophys 248: 53–61
22. POPE AJ, RA LEIGH 1987 Some characteristics of anion transport at the tonoplast of oat roots, determined from the effects of anions on pyrophosphate-dependent transport. Planta 172: 91–100
23. REA PA, CJ GRIFFITH, MF MANOLSON, D SANDERS 1987 Irreversible inhibition of $H^+$-ATPase of higher plant tonoplast by chaotropic anions: evidence for peripheral location of nucleotide-binding subunits. Biochim Biophys Acta 904: 1–12
24. REA PA, RJ POOLE 1985 Proton-translocating inorganic pyrophosphatase in red beet (*Beta vulgaris* L.) tonoplast vesicles. Plant Physiol 77: 46–52
25. ROTTENBERG H 1979 The measurement of membrane potential and $\Delta pH$ in cells, organelles and vesicles. Methods Enzymol 55: 547–569
26. SZE H 1983 Proton-pumping adenosine triphosphatase in membrane vesicles of tobacco callus: sensitivity to vanadate and $K^+$. Biochim Biophys Acta 732: 586–594
27. WANG Y, RA LEIGH, KH KAESTNER, H SZE 1986 Electrogenic $H^+$-pumping pyrophosphatase in tonoplast vesicles of oat roots. Plant Physiol 81: 497–502